Electron-Attachment Resonances of Glycine Zwitterions from Quantum Scattering Calculations: Modeling Macrosolvation Effects

I. Baccarelli,[†] A. Grandi,[†] F. A. Gianturco,*[,‡] R. R. Lucchese,[§] and N. Sanna[†]

Supercomputing Consortium for University and Research, CASPUR, Via dei Tizii 6b, 00185 Rome, Italy, Department of Chemistry, The University of Rome "La Sapienza", Piazzale A. Moro 5, 00185 Rome, Italy, and Department of Chemistry, Texas A&M University, College Station, Texas 77843-3255

Received: September 8, 2006; In Final Form: October 23, 2006

A computational study of the quantum dynamics for low-energy electrons scattered by the isolated zwitterionic species of the glycine molecule is carried out using a model interaction potential described in the main text. The macroscopic effects of water solvation on the target molecule in the electron scattering problem are described through a continuum polarizable model (CPCM) which modifies the target molecular structure. In such a way, realistic molecular orbitals depicting the glycine zwitterion in solution are used to model the electron−molecule interaction. The results of the calculations indicate the presence of five different transient negative ions (TNIs) formed at energies from the threshold and up to about 6 eV. Although no nuclear motion was explicitly considered in the ensuing decay processes, the analysis of the nodal structures and density distributions for the resonant excess electron wavefunctions over the molecular space suggests possible anionic fragmentations that produce $(Gly-H)^-$, H^-, $-CO_2^-$, and $-NH_3$. The likely consequences of such releases into the medium are briefly discussed.

I. Introduction

It has been suggested by a broad variety of experiments[1] that ionizing radiation which impinges on living cells can produce, among other species along the ionizing tracks, secondary electrons with kinetic energies in the 1−20 eV range and that such electrons constitute the main cause for DNA lethal lesions (i.e., single- and double-strand breaks (SSB and DSB, respectively)).[2] It is also interesting to note that the secondary electrons do not need to have energy in excess of DNA's ionization thresholds (10−25 eV) to induce such SSB and DSB processes.[3]

In a series of theoretical studies on DNA's bases, we have analyzed the theoretical and computational aspects of the scattering dynamics which is initiated by the secondary electrons on gas-phase specimens of uracil,[4] glycine,[5] and formic acid,[6] together with the analysis of higher-energy resonances observed on film-deposited uracil.[7] In the above studies, quantum scattering calculations of several resonant states located the presence of a broad variety of transient negative ions (TNIs) which could then be described as acting as "doorway" states or resonant precursors to the dissociative pathways induced by the metastable electron attachment to the target molecule.

Since the experiments which triggered the above analysis were nearly all carried out in the gas phase,[3,8,9] it therefore became useful to also develop the theoretical modeling in terms of single-collision processes triggered by the slow electron interacting with one target molecule in its ground electronic and internal energy state ($T = 0$ approximation). It is well-known, however, that the damaging effects of the secondary electrons mostly occur in the biological environment of an aqueous solvent, and therefore, it becomes important to further try to model the electron dynamics with partner molecules which have been modified by the solvation effects, given the established knowledge that individual aminoacids exist as cations in acidic media, charge-neutral zwitterions at intermediate pH values, and as anions in basic solutions. Five of the 20 aminoacids present also lateral charged functional groups whose charge state and, hence, whose properties are again determined by the pH value of the ambient solution. This marked dependence on the pH of the medium is transferred to the proteins which can be built from individual aminoacids and can bear important consequences on their behavior. Such changes, in fact, can alter protein shape and reactivity which in turn have dramatic consequences on their biological action.[10,11] In the context of the radiation damage problem, one could thus have to deal with additional secondary (damaging) effects whenever the fragments produced in the dissociative electron attachment (DEA) process are capable to macroscopically change the pH of the medium.

As a first step toward the modeling of peptides in solution, we present here the study of the DEA processes limited to one single aminoacid in aqueous medium; our main concern is to combine a realistic description of a molecule in solution with our treatment of electron−molecule scattering before moving to the simplest oligopeptides. Obviously enough, the results on the likely fragmentation patterns following the electron attachment step will, eventually, concern the terminal parts of a protein chain and therefore do not represent here the modeling of a peptide in solution. However, it is a necessary starting point in the tuning of our computational scheme in a *non-gas-phase* environment.

As already mentioned, since biological systems are almost universally in aqueous solutions, the isolated aminoacids (which are strictly neutral in the gas phase) take the form of zwitterions in the condensed phase and exist in a wide variety of charge states with different relative populations depending on the pH

* Author to whom correspondence should be addressed. Fax: +39-06-49913305. Electronic mail: fa.gianturco@caspur.it.
[†] Supercomputing Consortium for University and Research.
[‡] The University of Rome "La Sapienza".
[§] Texas A&M University.

10.1021/jp065872n CCC: $33.50
Published on Web 12/07/2006

of the ambient solution and on the spatial locations of the relevant counterions around the zwitterionic species.

In the present analysis, we therefore wish to study the differences in behavior of the most likely fragmentation patterns for one of the simplest aminoacids, the glycine molecule, when the latter is considered to exist in its zwitterionic form as an example of one of its more common charge states at intermediate pH values.[10] In particular, having already analyzed the fragmentation following electron attachment processes in the gas phase on the glycine canonical structures[5] as discussed by experiments,[8] we will show in the following that a similar dynamical modeling could be carried out in order to identify possible TNI states and possible molecular fragments which would be released into the solution environment after the electron impact process. The basic idea is still that of limiting the dynamical study to its initial fast step during which the impinging electron is not yet thermalized by multiple scattering off the solvent molecules but instead generates directly the TNI structures which will eventually be released into the aqueous solution. In other words, we will be disregarding for the time being the solvent capability of creating microcaging around the solute targets (counterions), and the possible electron multiple scattering off such structures, while we shall include as realistically as possible the structural changes on solvated species which can be induced by the solvent in order to be able to carry out the scattering dynamics in a different situation from that of the gas phase.[5]

It should therefore be kept in mind that the "fast process" description we are adopting employs the COSMO enhanced polarized continuum medium (CPCM) to generate electronic effects (see section II for details) only on the target molecule, with the scattered electron indirectly sampling such effects through the changes in the target structure itself. Hence, the additional counterfield created by the polarized medium in the volume occupied by the target molecule will only affect the relative velocity of the electron with respect to the target and, therefore, the ensuing background cross sections, but not the (short-range) interaction forces between the projectile and the molecule which are directly responsible for the TNIs formation. In other words, the only essential solvent effect which has to be taken into account in our modeling of the resonant processes in the zwitterion species consists of the solvent-induced modifications of the target bound molecular orbitals. Thus, we claim here that, within our usual level of approximation concerning the fixed nuclei description and the chosen model correlation and exchange interactions which we shall be describing below, we are indeed dealing with electron scattering off a solvated molecule, the latter picture relying on the mature methodology of the CPCM description of the macroscopic solute molecule.[12]

In the following section, we shall briefly discuss the structural features of the zwitterion of the glycine aminoacid, while section III will summarize our dynamical model. The results of our calculations will be given in section IV, while section V will finally provide our present conclusions.

II. Glycine Zwitterion

All of the common, naturally occurring aminoacids can form zwitterions in solution because of the stabilizing effects of solvation *via* counterion production.[13,14] On the other hand, it also seems to have become clear that none of these aminoacids can form zwitterions as isolated, gas-phase molecules.[15−17] For the case of glycine, recent calculations have looked into the possibility that electron attachment to the isolated molecules could preferentially stabilize the zwitterionic structure by the formation of dipole-bound anionic states[16] but argued that it was not the case. More recent experimental studies of the arginine system[17] concluded that, in this case, because of this aminoacid's much larger proton affinity, the zwitterionic structure could be competitively stabilized with respect to the canonical structure because of the dipole attachment of the extra electron after protonation. It does not seem likely, however, that zwitterionic forms of the aminoacids could become stable in the gas phase when undergoing electron attachment processes.

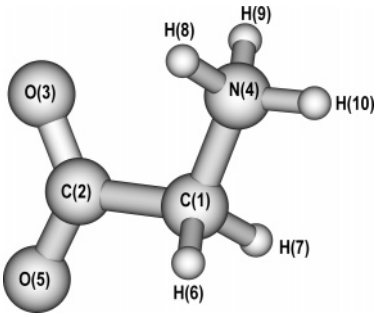

Figure 1. Optimized structure of the glycine zwitterion from CPCM stabilization.[19]

We have already carried out stable structure calculations for the isolated, canonical structures in the gas phase,[5] and as mentioned in the Introduction, we have repeated the same calculations by also stabilizing the new zwitterionic structure with the use of the polarized continuum model[18] for the water solvent in the COSMO enhanced version (CPCM),[12] as implemented in the GAUSSIAN package.[19] The structure of the most stable zwitterion, calculated at the HF/6-31G(d) level, is shown by Figure 1, where the labeling of the various atoms of glycine is also shown. No attempts were made at recalculating the scattering process for different structures as we already know from earlier studies that although resonant features are dependent on the structural details[6] and, therefore, one expects the present results to hold within the reliability of the optimized structure shown in Figure 1, the general qualitative picture does not usually change.

PCM-related methods are widely used (with more than 1000 papers published in international journals) and proven to be reliable in order to describe structural as well as dynamical properties of molecules in solution. In particular, one of the first applications of the PCM method concerned the conformations and energy of canonical and zwitterionic forms of glycine arriving at a value of the free energy difference between the two forms very near to the best estimates without the need of introducing explicitly the caging water molecules in the model.[20] Although the polarized continuum models do not include hydrogen bonding and, in this sense, the PCM description of a molecule in solution is an approximated one, it has been proven to be an excellent approximation, capable of reproducing the features of the solvated system. Furthermore, since in the present work we focus on the effects induced by the solvation medium on the dissociation paths following electron attachment to the glycine molecule, we are not considering that the water molecules surrounding the solute can themselves undergo DEA processes with the formation of TNIs where the excess electron is localized on the water molecule[23] because this is a different process with respect to the fragmentation of the zwitterion. We might also think (in a speculative fashion) of possible additional resonant features arising from the formation of a TNI delocalized between the solute and one (or more) individual water molecules of the first shell of solvation, and again, this would be a different

TABLE 1: Mulliken Computed Net Charges on the Optimized Structures of the Glycine Canonic Species of the Gas Phase (3rd Column) and the Zwitterionic Form from CPCM Solvent Stabilization (4th Column)[a]

atom	label	isolated canonical structure	zwitterion
C	1	−0.23	−0.31
C	2	0.71	0.76
O	3	−0.56	−0.77
N	4	−0.82	−0.84
O	5	−0.69	−0.78
H	6	0.21	0.25
H	7	0.21	0.25
H	8	0.35	0.48
H	9	0.35	0.48
H	10	0.47	0.48

[a] The atom labeling is that of Figure 1.

process involving the complex $Gly-(H_2O)_n$. What we want to study instead is the possible differences induced in the fragmentation patterns following the localization of the excess electron on the glycine molecule once it is embedded in an aqueous medium. To this aim, what we have to care about is limited to a correct representation of the glycine molecular orbitals (MOs) which are modified by the interaction with the solvent. Hence, we are aware that the present exploratory work does not constitute as yet a "complete" study of a zwitterionic glycine in solution and that possible experiments could provide a more complex picture deriving from many other processes which can take place whenever a beam of electrons transverses a solution of glycine molecules. However, if the CPCM description of a molecule in solution is accepted as reliable, as already attested in the current literature,[18,20] our approach to study those selected TNIs which are localized on the molecule indeed provides a useful piece of information whenever the interpretation of future experimental findings arising from the complex interplay of many effects shall be carried out.

We further note that we had already analyzed in some of our previous work[24] the effects of resonant states formation on a model N_2 molecule "caged" in small clusters of Ar atoms and had indeed found the presence of at least two types of TNIs: those where the electron is localized on the N_2 molecule (thus modeling the caged N_2^- resonances) and those where the extra electron is captured by the "solute" Ar atoms (the Ar^- resonances). In analogy with the latter modeling, we are here focusing on the $(Gly)^-$ resonances only. Our arguments were somehow implicitly adopted in the work of Simons and coworkers;[21,22] in a series of papers aiming to unravel the mechanism for damage to DNA by low-energy electrons by means of ab-initio electronic structure calculations, the authors employed the PCM solvation model in order to describe the effect of surrounding water molecules on the electronic energy and geometry of their model DNA fragments and TNIs.

The relevant net charges calculated by Mulliken's population analysis are given by Table 1, which follows the numbering of the atoms shown by Figure 1, and we compare the net charges obtained from the lowest canonical isolated structure with those given by the zwitterion calculations. One clearly sees there that such changes are fairly small and chiefly involve the C(1) atom and one of the C═O oxygens, the O(3), while little happens to the nitrogen that now carries the three H atoms, N(4), since the positive charge markedly migrates onto those hydrogen atoms (as opposed to the ones forming the CH_2 terminus), a feature which is expected to be present in a zwitterionic species.

To further clarify the stabilization effects on the zwitterionic structure provided by quantum chemical calculations of the corresponding anion,[16] we report in Figure 2 the lowest unoccupied molecular orbital (LUMO) obtained from the zwitterion calculations. The symmetry is A', i.e., we are dealing here with a σ^*-like orbital, and clearly see its chief location on the oxygen atoms and on the C(1) carbon atom, with antibonding features across the N(4)−C(1) bond. As we shall see later on, this virtual orbital turns out to be only vaguely similar to the localization shown by the resonant excess electron in specific TNIs that we shall obtain from the scattering calculations of the present work and its energy location is also different from that given by the scattering calculations. Hence, we argue that the zwitterionic TNIs formed from scattering processes are not well described by employing the above LUMO to obtain a picture of the extra, metastable electron of the resonant complex.

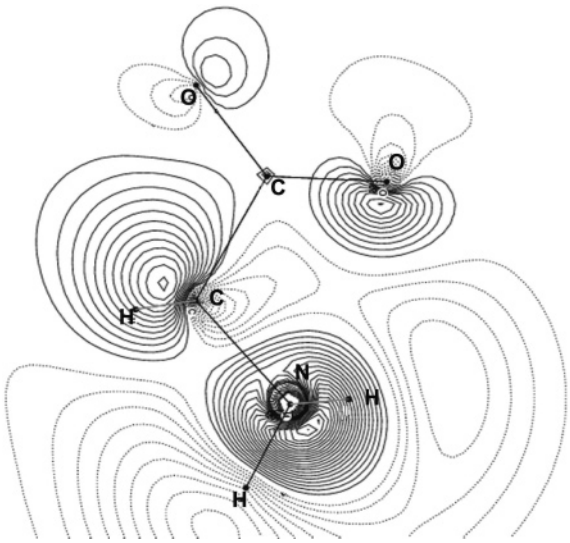

Figure 2. Computed probability density for the LUMO of the zwitterionic form of glycine. Its energy location is at $E = 5.36$ eV, and the symmetry is σ^* (A'). Notice that in this figure, as well as in the following ones, the two out-of-plane hydrogen atoms at the C(1) and the N(4) sites (see Figure 1) overlap in the projection on the chosen xy plane.

III. Scattering Model

Within the Born−Oppenheimer (BO) approximation, one represents the total wave function of the system with one electron scattered from an N-electron molecular target as an antisymmetrized product of $(N + 1)$ electron wave functions that parametrically depend on the nuclear coordinates. Since the present treatment of the scattering process is limited to an analysis of the elastic channels, no excitations will be considered for either the bound electrons or the bound nuclei (see our recent review, ref 25, for a lengthy discussion on the method we employ). The description of the electronic wave function for the zwitterion will be given as a single-determinant of Hartree−Fock quality MOs describing the N-bound electrons. To obtain our scattering equations, we then expand both the bound MOs and the continuum electron in a single-center expansion (SCE) around the center of mass of the target via symmetry-adapted angular functions. If one then writes down the scattering state as the product of a one-electron scattering function and a single-determinant target wave function, one obtains the static-exchange representation of the electron−molecule interaction for the ground state. Additionally, to reduce the computational task, we have replaced the exact nonlocal exchange interaction with an energy-dependent local exchange potential[26,27]

$$V_{ex}^{FEGE}(r) = \frac{2}{\pi}k_F(r)\left(\frac{1}{2} + \frac{1-\eta^2}{4\eta}\ln\left|\frac{1+\eta}{1-\eta}\right|\right) \quad (1)$$

where $\eta(r) = [(k^2 + 2I_p + k_F(r))^{1/2}]/[k_F(r)]$, $k_F(r) = (3\pi^2\rho(r))^{1/3}$ is the local Fermi momentum, and I_p is the ionization potential of the molecular target.

In the present approach we include the effects of the additional dynamical short-range correlation forces through a local energy-independent potential V_{corr}.[26,28] The V_{corr} potential is obtained *via* the average dynamical correlation energy of a single electron within the formalism of the Kohn and Sham variational scheme (for details, see also refs 28 and 29). The functional derivative of such a quantity with respect to the self consistent field (SCF) *N*-electron density of the molecular target provides a density functional description of the required short-range correlation term, this being an analytic function of the target ground-state electron density. When studying the full scattering problem, we correct the large *r* behavior of V_{corr} so that it agrees with the known static polarizability of the target molecule,[26] although in the present study we are chiefly interested in locating the TNIs of the system which correspond to well-localized scattering states. Hence, they are not usually affected by the shape of the long-range forces that are, however, essential for producing the correct background phase contributions to yield total cross sections, especially at energies close to the threshold. In other words, to correctly generate the full interaction within 12 Å from the molecular center of mass, it is sufficient to realistically describe the "localized" scattering states which give rise to solvated TNI species, which in turn are largely unaffected by the inclusion of long-range polarization forces.

To examine in some detail the mechanism and qualitative characteristics of low-energy, one-electron resonances, we further employ a model which is simple enough to be computationally attractive but with sufficient details of the full scattering problem to reproduce the essential features of the realistic cases. Hence, to facilitate the analysis of the resonances, we have used an adiabatic representation of the electron−molecule interaction potential.[26] Since the standard, symmetry-adapted angular momentum eigenstates do not form the most compact angular set for the electron−molecule scattering problem, we have used an alternative expansion basis by diagonalizing the angular Hamiltonian at each radius *r*. These new angular eigenstates are the adiabatic angular functions which are distance-dependent, linear combinations of the symmetry-adapted *asymptotic* harmonics. The eigenvalues of the angular Hamiltonian then form an adiabatic radial potential over the selected range of the e^-−molecule distance.

To describe the nonadiabatic coupling terms, we employ a piecewise diabatic (PD) representation for the potential[26,30] where the radial coordinate is divided into several regions so that sector *i* is defined as $r_{i-1} < r < r_i$, with $r_0 = 0$. In each region, we average the coupling potential over *r* and the resulting averaged potential is diagonalized to yield a set of angular functions. Solving the radial equations using this approach requires matching of the radial functions and their derivatives at the boundary between radial regions. The scattering was then solved within the reduced basis of the effective diabatic potential terms, and the corresponding poles of the **S** matrix have been obtained in the energy range of experimental interest, i.e., from the threshold to about 15 eV.

A. Transient Molecular Ion (TNI) Calculations. To obtain the resonant states, the poles of the **S** matrix were computed using 70 radial regions including PD potential terms up to $l = 12$ (including 91 radial functions for the A' symmetry component and 78 for the A'' symmetry component, within the C_S symmetry of the target molecule). The bound target electrons were computed at the 6-31G(d) quality of basis set expansion.[19]

The mapping of the A' resonant states was done in the plane of the molecule, while the A'' TNI states have been mapped in a plane which is located at $0.75a_0$ above the molecular plane since these are π-like states which have a nodal surface in the plane of the molecule. The calculations of the potential were carried out up to $l_{max} = 80$ for its initial multipolar expansion, while the scattering wave functions included partial waves up to $l_{max} = 40$. The V_{corr} was obtained from the density functional theory (DFT) formulation discussed before.[26] The radial integration was carried out up to $r_{max} = 12a_0$, whereby the energy locations and widths of our resonant states were deemed to be numerically converged to within 10% of their values.

TABLE 2: Computed Energy Positions and Widths (in electronvolts) of All the Transient Anionic States of the Glycine Zwitterion in Both Contributing Irreducible Representation (IRs) of the C_S Symmetry

IR	E_r (eV)	Γ_r (eV)	IR	E_r (eV)	Γ_r (eV)
A'	0.59	0.16	A''	0.87	0.06
	1.38	0.10		6.32	1.64
	5.83	1.04			

IV. Present Results

The results collected in Table 2 summarize the locations and widths of the resonances obtained from the present study. We report, there, only those poles of the **S** matrix which were deemed to correspond to physically plausible resonances, i.e., resonant states with lifetimes long enough to provide widths that were more likely to be detected, i.e., widths up to about 1 eV of the imaginary energy components for the corresponding poles. One therefore sees that the table reports five resonances, three of A' (σ^*) symmetry and two of A'' (π^*) symmetry.

A. Spatial Mapping of Resonant Electrons. When strong (efficient) dynamical trapping of the scattered electron occurs during the collision, then the corresponding continuum wavefunction undergoes marked spatial localization in regions close to the scattering center. In our case, therefore, the target molecule center of mass constitutes the reference center for defining such localization effects. It therefore follows that the mapping of the scattered wavefunctions for the $(N + 1)$ electrons over the spatial region of the nuclear network can help us to define specific features of that metastable particle which in turn can guide us in the understanding of the ensuing DEA processes. One interesting difference from the computed results of gas-phase isolated glycine[5] is the presence of uniformly narrower resonances located at much lower energies when the zwitterionic structure is considered: only a A'' resonance around 3 eV was seen in the gas-phase calculations,[5] while now we see it here as splitting into a threshold resonance at 0.87 eV (with a very long lifetime) and a broader resonance around 6 eV. Furthermore, the σ^* (A') resonances of the glycine molecule in its canonical form were all placed at somewhat high energies (between 8 and 12 eV) and were also fairly broad ($\Gamma > 1$ eV). We see instead that the isolated zwitterionic target exhibits three resonances at much lower energies (from the threshold and only up to 6 eV) and associated with longer lifetimes (see Table 2). One therefore observes that the stronger charge localization effects which are present in the zwitterionic structure act more efficiently on the formation and stabilization of the TNIs during the scattering process. The much stronger polar structure, in fact, interacts with the impinging electron over a greater range of radial regions and, qualitatively speaking, brings the reso-

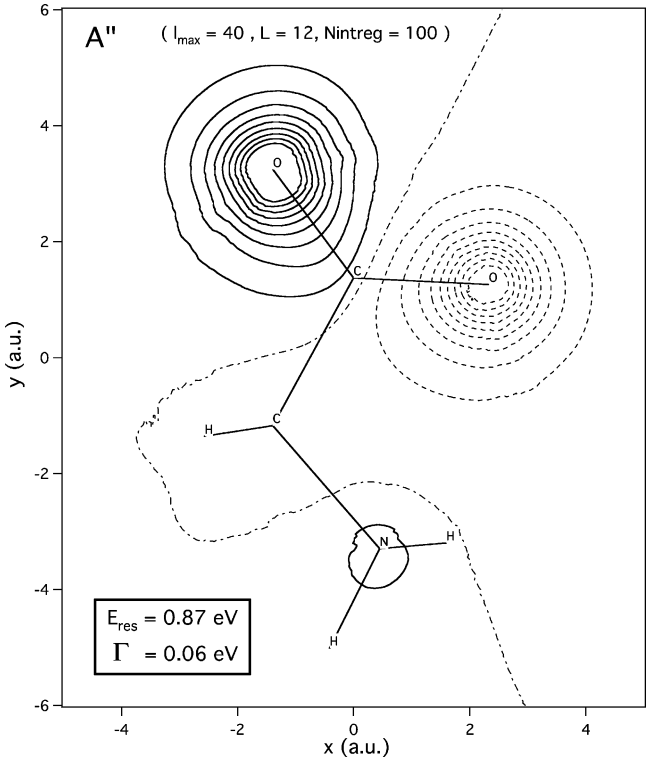

Figure 3. Spatial distribution of the excess electron wavefunction associated with the π^* resonance at 0.87 eV. The mapping is drawn at $0.75a_0$ above the nodal plane.

nances closer to their thresholds. This result is in keeping with recent quantum calculations of thymine solvated by a few water molecules[31] where the weakly bound anionic species were found to become more bound as the number of added molecules increased. Thus, we see here that the π^* (A'') resonance is now moved down to 0.87 eV and becomes very narrow, as opposed to the behavior of the glycine in its canonical form, where calculations located only one π^* resonance around 3 eV.[5] The spatial distribution of this A'' resonant orbital from the present calculations is shown in Figure 3.

One immediately notices that no excess charge is located on either the H atoms attached to the carbon or those attached to the nitrogen atom. Hence, it is reasonable to expect that those bonds, when involved with the excess electron energy rearrangement within the system, may undergo dissociation as neutral fragments, leaving the excess charge onto the main molecular residue: it would thus be the $(Gly-H)^-$ species also detected above 1 eV in the gas-phase mass spectra of the canonical counterpart but appearing in the zwitterionic form much closer to the threshold.

This excess electron therefore corresponds to the attachment of a temporary electron to a π^* orbital of what is the $-COOH$ group in the gaseous glycine. The electron transmission spectroscopy (ETS) experiment on glycine[32] canonical, gas-phase samples located, in fact, this state at around 1.93 eV, and our earlier calculations on the same system[5] confirmed such a resonance around 3 eV, the difference with the experiment being due there to our use of a local model potential.[5] The present zwitterionic form shows a marked lowering of the resonance to below 1 eV, as seen in the data of Figure 3. We, therefore, suggest here that a possible change due to the solution environment could be the observational appearance of a $(Gly-H)^-$ peak much closer to the threshold than that seen in the gas-phase experiments. Hence, one may even envisage that such resonant fragmentation may not be seen in the solution

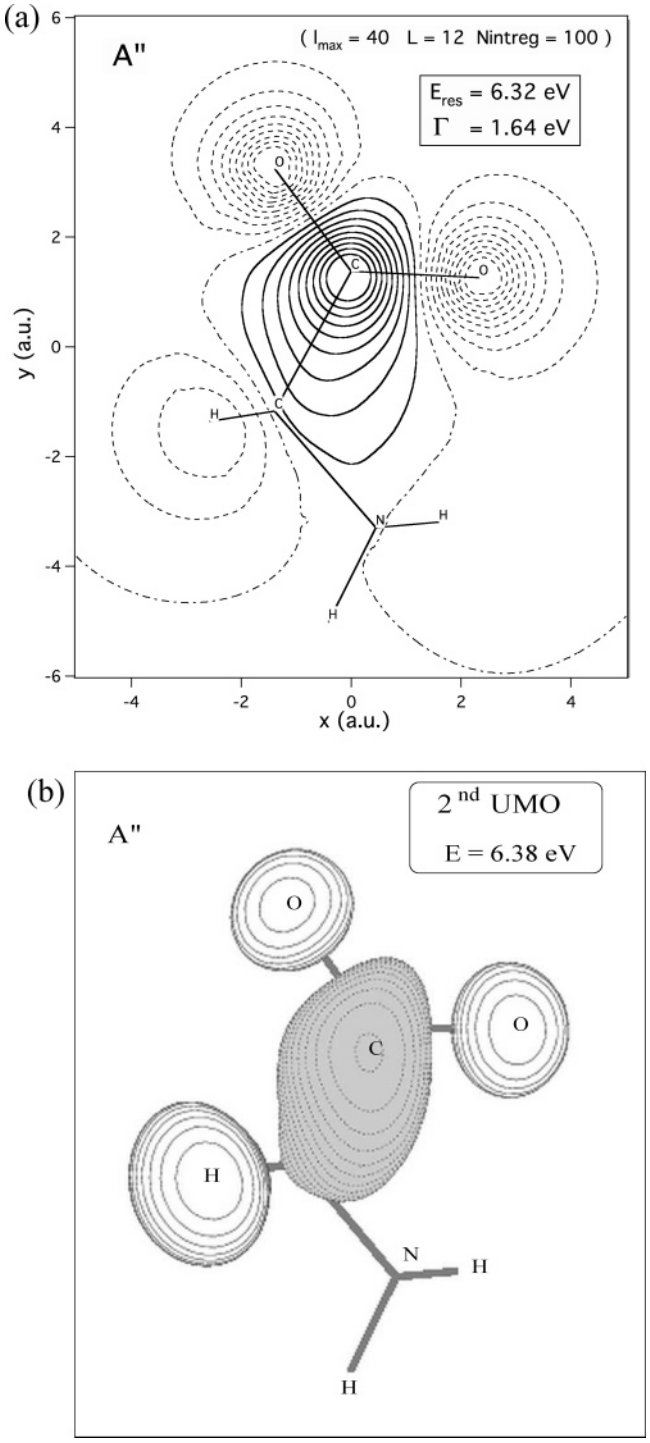

Figure 4. (a) Computed excess electron isodensity map for the higher-energy A'' resonance reported in Table 2. (b) LUMO + 1 orbital (A'' symmetry). The mapping of the MO in panel b has been obtained directly from the output of the GAUSSIAN code.

environment where the solvent caging effects may prevent this slow, resonant electron from leaving the zwitterion target by forming new, stable anions of glycine.[31]

The second A'' (π^*) resonance exhibited by the zwitterionic species is located at much higher energies, i.e., around 6 eV, and turns out to be much broader than the threshold attachment resonance (see Table 2). The spatial distribution of the excess electron wavefunction is shown by Figure 4a, where the isodensity curves are plotted above the nodal plane which cuts across the CH_2 group. If we now look at Figure 4b, where we report the (LUMO + 1) orbital with the same symmetry

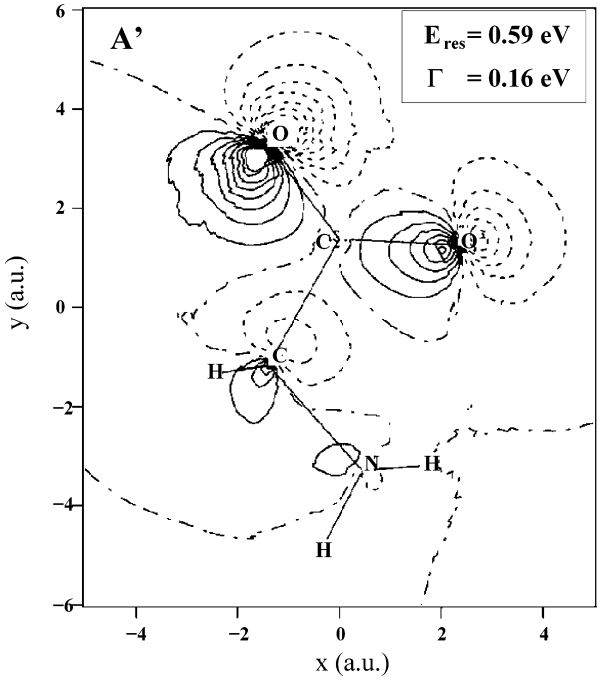

Figure 5. Computed density isolines, on the molecular main symmetry plane, shown for a resonant electron located at 0.59 eV of *A′* (*σ**) symmetry.

generated by the SCF calculations for the zwitterionic target, we discover an uncanny similarity of its spatial shape with that of the scattered electron given in panel a. This seems to be one of the cases, often found by us in previous work,[4,7] where the virtual space mapped by the SCF orbitals produces anionic states which turn out to be very similar to actual scattering states. However, there is no real way of selecting them in advance without doing the more realistic scattering calculations, as we did in the present system.

One marked difference from the gas-phase situation is that we did not find for it[5] a higher-energy, broad *π** resonance as the one shown here. Furthermore, the resonant electron density is now clearly present on the H atoms of the $-CH_2$ group and on the carbon atom of the $-CO_2$ group: the nodal plane across the −CH bonds additionally suggests that such a higher resonance could provide H^- detachment upon fragmentation, a possible experimental signal which was not at all present in the gas-phase species but which is shown here by our calculations to be more likely to occur for the zwitterionic molecule. With the same token, and depending on the internal vibrational rearrangement (IVR) efficiency of such short-lived TNI, we can also say that the antibonding planes across the C−O bonds suggest possible release of O^- fragments at these high energies.

If we now extend the density analysis to the *σ** resonances, we see that Table 2 indicates the presence of three of such resonances (as was the case for the canonical, gas-phase glycine[5]) but all located at much lower energies and with longer lifetimes than those computed for the aminoacid in its canonical form: the zwitterionic structure, therefore, is seen to both lower the resonance energies and to lengthen their corresponding lifetimes.

Figures 5 and 6 show the computed isodensity lines for the two lower *σ** resonances located at 0.59 and 1.38 eV, respectively, and with corresponding widths of a few milielectronvolts. The next, higher energy *A′* resonance, located at nearly 6 eV and with a much broader width, is shown by the map of Figure 7.

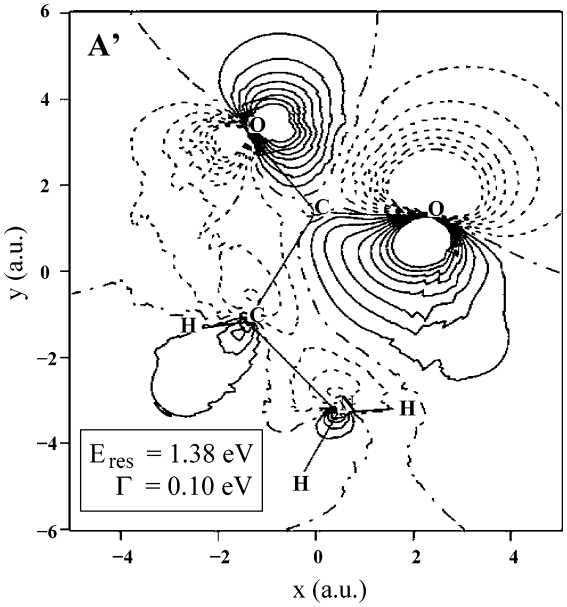

Figure 6. Same plot as in Figure 5 but for the next *A′* (*σ**) resonance located at 1.38 eV.

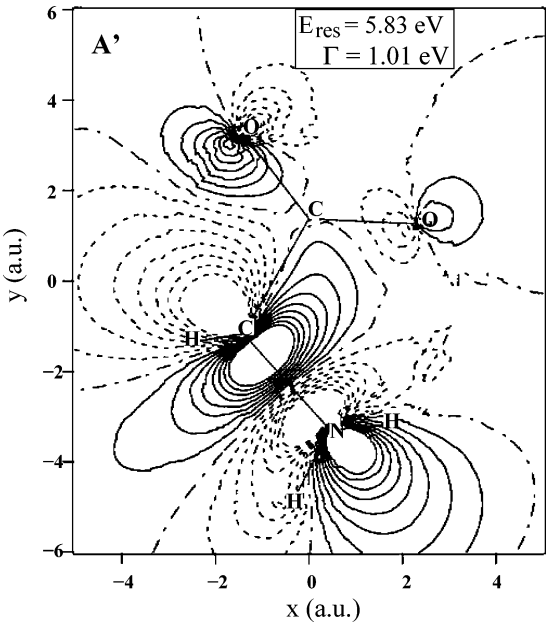

Figure 7. Computed excess electron wavefunction isolines for the *σ** resonance at 5.83 eV reported in Table 2.

A perusal through the results shown by these figures clearly tells us that in both instances the excess electron density is higher over the oxygen atoms of the $-CO_2$ group, a feature which differs from the same symmetry maps associated with the canonical, gas-phase glycine of our previous calculations.[5] We showed there, instead, that it was the $-NH_2$ and the $-CH_2$ groups which were chiefly involved in those resonances and that the resonances were also located at much higher energies.

Since the present metastable electron maps further indicate that the lowest resonance of *σ** symmetry of Figure 5 does not exhibit any excess electron charge onto the $-CH_2$ or $-NH_3$ hydrogen atoms, we surmise that the latter could give rise to the possible release of $[Gly-H]^-$ anionic species into the solution, with the H atom detachment after resonance decay as already suggested for the threshold *π** resonance discussed before. Such a possibility would therefore either increase the probability of H atom detachment, with the formation of

$[Gly-H]^-$ anions in the solution, or would be quenched by secondary solvent binding effects on the threshold electron as discussed before. The presence of either outcome will thus depend on the relative electron affinity of the threshold electron between the TNI species and the solvent molecules and also on the actual concentration of the solute molecules in the examined solution.

The nodal structure of the next σ^* resonance reported by Figure 6 also indicates excess electron density on the $-CO_2$ functional group, but it further shows marked antibonding planes across the C−C central bond: it therefore suggests energy rearrangement paths within the zwitterion that could lead to the release of $-CO_2^-$ species into the surrounding ionic solvent. A sufficient concentration of such TNIs would therefore macroscopically modify the existing pH conditions of the solution and thus change the aminoacid structure.

We next move to the highest σ^* resonance located around 6 eV and show its wavefunction density isolines for the excess electron by the map of Figure 7. The situation is now markedly different from the ones reported by Figures 5 and 6: the excess electron wavefunction has now moved onto the $-CH_2$ and, even more, onto the $-NH_3$ zwitterionic fragments. Furthermore, the marked antibonding character across the H_2C-NH_3 bond indicates the clear possibility of internal energy rearrangements by fragmentation with nearly neutral $-NH_3$ release into the ambient solvent: again, this suggests the possibility of changing the solution pH through a mechanism nanoscopically induced by dissociative electron attachment processes.

It is interesting to note, at this point, that a recent theoretical model[22] for electron attachment to biosystems has argued about the presence of direct dissociative attachment processes whereby the metastable electron induces the presence of a molecular anion which is dissociative along the bond where the electron is chiefly located, while the indirect DEA processes would correspond to bond-breaking in a different molecular *region.* The present search of doorway states by examining the molecular features of scattering electrons follows a very similar philosophy: we argue that nodal structures across specific bonds suggest that this particular TNI would be likely to undergo molecular dissociation in a direct manner by guiding bond rupture *via* those antibonding characteristics of the excess electron wavefunction. With the same token, we also suggest that finding molecular regions which are void of excess electron density (while others carry instead most of that resonant electron density distribution) is equivalent to locating the presence of an indirect dissociation mechanism whereby the attached electron preferentially populates specific molecular bonding areas while other bonds are not strengthened by this "force constant's enrichment" effect and therefore could more easily respond to internal vibrational redistribution of the excess electron energy. The net consequence of that specific TNI would therefore be indirect molecular dissociation with electron attachment to the one residual fragment on which it was initially localized. In other words, our present analysis of the spatial and nodal features of the metastable electron is meant to provide, albeit at the qualitative level, the distinction between direct and indirect mechanisms surmised by the analysis of ref 22.

V. Present Conclusions

In this work, we have carried out a sort of computational experiment on electron scattering off the zwitterionic states formed by the glycine molecule in aqueous solutions.

In particular, we have looked at the possible metastable anionic states (TNI states) that could occur *via* direct low-energy electron attachment to the zwitterion and at the fragmentation patterns which are caused by the formation of such doorway states and which may lead to dissociative electron attachment processes into the environment.

In modeling the dynamical fragmentation, we have not looked at the possible role of those electrons which are being multiply scattered by the molecular network of the aqueous solute: the studies on radiation damage mechanisms, in fact, suggest[1−3] that the lifetime of slow electron deceleration by the water environment after the primary ionization process, an energy loss which leads eventually to solvated electrons into the medium,[33] is much longer than the DEA process which we are considering. This means that the effect of zwitterionic formation could be modeled as being chiefly a structural change of the target molecule induced by the water solvent, without the explicit inclusion of the water molecules themselves either as active scattering sites during the electron attachment process or via their structural effects on the scattering potential by the locations of the counterions or of the CPCM charges. Indeed, the present study is entirely directed to the analysis of electrons primarily scattered by the zwitterionic target.

Following the above philosophy, we have therefore analyzed the formation of transient anionic species by electron attachment to the zwitterion taken by itself and have looked at the spatial features of the five resonant states which we have obtained from calculations, comparing them with the different results, both from experiments and calculations, that had been obtained on the canonical gas-phase glycine.

Our present modeling suggests the following differences with the earlier gas-phase findings:

(1) Due to the presence of a marked polar structure within the zwitterionic species (*vis á vis*, the canonical glycine molecule), all resonances are shifted to lower energies because of the increased strength of the charge−dipole interaction contribution.

(2) The zwitterionic species shows efficient formation (long lifetimes) of two TNI states of σ^* and π^* character near the threshold, both indicating the likelihood of producing bond-breaking pathways with losses of an H atom. In other words, as it occurs with canonical glycine, one should have H atom losses in solution also and they should occur at lower electron energies. In case the solvent molecules are capable of preventing the escape of those threshold electrons by stabilizing such anionic structures, however, one may not see such losses detected in experiments.

(3) Differently with what was found for the isolated glycine target, the new calculations also suggest the presence of a higher energy resonance around 6 eV where the extra electron gets located onto one of the H atoms and therefore suggests a bond-breaking pathway whereby the H^- species is formed. Such a dissociation product was not observed (either experimentally of theoretically) for canonical glycine. The same TNI could also provide the detachment of O^- fragments into the solution.

(4) The remaining two resonances of A' (σ^*) symmetry indicate the possible presence of fragmentation pathways leading to the release into the solution of CO_2^- and NH_3 fragments. Since both species, if present with sufficiently large concentrations, would macroscopically change the pH of the relevant environment, it would be interesting to see from experiments how much the DEA macroscopic rates would be able to create such noticeable changes. As far as we know, no estimates exist for these rates, so our suggestion remains at the conjectural level only. However, these two resonances point at possible fragmentation results which would enhance the damaging effect by

creating a different chemical environment for the remaining zwitterionic biomolecules.

No electron-scattering experiments exist, as far as we are aware, on the present system in solution. However, this preliminary computational study (the first of this kind) provides specific indications for marked differences to occur in the fragmentation process, once the "solvated" target molecule is considered instead of the simpler gas-phase system.[8] It also suggests an explanation at the nanoscopic level of what may be the molecular causes for such differences: we hope that our present findings will be able to trigger further experimental searches on the behavior of zwitterionic species under low-energy electron bombardment.

Acknowledgment. The financial support of the University of Rome I "La Sapienza" Research Committee, of the CASPUR Consortium computing facilities, and of the European Research Network EPIC no. HPRN-CT-2002-00179 is gratefully acknowledged. F.A.G. and R.R.L. are grateful for the support from a NATO collaborative Research Grant (no. PST.CLG.978702). F.A.G. is thankful for the Von Humboldt Prize, and R.R.L. acknowledges the Welch Foundation, Grant No. A-1020. We also wish to thank Mr. Marco Campetella for his enthusiastic help with the initial zwitterionic structure calculations and Dr. A. Grottesi for helpful discussion.

References and Notes

(1) For example, see: Sanche, L. *Mass. Spectrom. Rev.* **2002**, *21*, 349−369.

(2) Pimblott, S. M.; LaVerne, J. A. In *Radiation Damage in DNA: Structure/Function Relationships at Early Times*; Fuciarelli, A. F., Zimbrick, J. D., Eds.; Battelle: Columbus, OH, 1995; p 3.

(3) Abdoul-Carime, H.; Cloutier, P.; Sanche, L. *Radiat. Res.* **2001**, *155*, 625−633.

(4) Gianturco, F. A.; Lucchese, R. R. *J. Chem. Phys.* **2004**, *120*, 7446−7455.

(5) Gianturco, F. A.; Lucchese, R. R. *J. Phys. Chem. A* **2004**, *108*, 7056−7062.

(6) Gianturco, F. A.; Lucchese, R. R. *New J. Phys.* **2004**, *6*, 66

(7) Grandi, A.; Gianturco, F. A.; Sanna, N. *Phys. Rev. Lett.* **2004**, *93*, 048103.

(8) Ptaskinska, S; Denifl, S.; Abedi, A.; Scheier, P.; Maerk, T. D. *Anal. Bioanal. Chem.* **2003**, *377*, 1115.

(9) Gohlke, S; Rosa, A.; Illenberger, E.; Brüning, F.; Huels, M. A. *J. Chem. Phys.* **2002**, *116*, 10164−10169.

(10) Gordon, M. L.; Cooper, G.; Morin, C.; Araki, T.; Turci, C.; Kaznatcheev, K.; Hitchcock, A. P. *J. Phys. Chem. A* **2003**, *107*, 6144−6159.

(11) Messer, B. M.; Cappa, C. D.; Smith, J. D.; Wilson, K. R.; Gilles, M. K.; Cohen, R. C.; Saykally, R. J. *J. Phys. Chem. B.* **2005**, *109*, 5375−5382.

(12) Cossi, M; Rega, N.; Scalmani, G.; Barone, V. *J. Comput. Chem.* **2003**, *24*, 669.

(13) Wyttenbach, T.; Witt, M.; Bowers, M. T. *J. Am. Chem. Soc.* **2000**, *122*, 3458−3464.

(14) Price, W. D.; Jockusch, R. A.; Williams, E. R. *J. Am. Chem. Soc.* **1997**, *119*, 11988−11989.

(15) Rak, J.; Skurski, P.; Simons, J.; Gutowski, M. *J. Am. Chem. Soc.* **2001**, *123*, 11695−11707.

(16) Gutowski, M.; Skurski, P.; Simons, J. *J. Am. Chem. Soc.* **2000**, *122*, 10159−10162.

(17) Xu, S.; Zheng, W.; Radisic, D.; Bowen, K. H., Jr. *J. Chem. Phys.* **2005**, *122*, 091103.

(18) Tomasi, J.; Mennucci, B; Cammi, R. *Chem. Rev.* **2005**, *105*, 2999.

(19) Frisch, M. J.; Trucks, G. W.; Schlegel, H. B.; et al. *Gaussian 03*, revision C.02; Gaussian, Inc.: Wallingford, CT, 2004.

(20) Bonaccorsi, R.; Palla, P.; Tomasi, J. *J. Am. Chem. Soc.* **1984**, *106*, 1945−1950.

(21) See, e.g., Barrios, R.; Skurski, P.; Simons, J. *J. Phys. Chem. B* **2002**, *106*, 7991−7994. Berdys, J.; Anusiewicz, I.; Skurski, P.; Simons, J. *J. Phys. Chem. A.* **2004**, *108*, 2999−3005. Berdys, J; Skurski, P; Simons, J. *J. Phys. Chem. B* **2004**, *108*, 5800−5805.

(22) Anusiewicz, I.; Sobczyk, M.; Berdys-Kochanska, J.; Skurski, P.; Simons, J. *J. Phys. Chem. A* **2005**, *109*, 484−492.

(23) For example, see: Gianturco, F. A.; Paioletti, P. In *Novel aspects in electron-molecule collisions*; Becker, K. H. Ed.; World Scientific: Singapore, 1998; p 57.

(24) Lucchese, R. R.; Gianturco, F. A. *J. Chem. Phys.* **1997**, *107*, 8483−8490.

(25) Baccarelli, I.; Gianturco, F. A.; Grandi, A.; Lucchese, R. R.; Sanna, N. *Adv. Quantum Chem.*, **2007**, *52*, in press.

(26) For example, see: Lucchese, R. R.; Gianturco, F. A. *Int. Rev. Phys. Chem.* **1996**, *15*, 429.

(27) Hara, S. J. *J. Phys. Soc. Jpn.* **1967**, *22*, 710.

(28) Perdew, J. P.; Zunger, A. *Phys. Rev. B* **1981**, *23*, 5048−5079.

(29) Lee, C.; Yang, W.; Parr, R. G. *Phys. Rev. B* **1988**, *37*, 785−789.

(30) Gianturco, F. A.; Lucchese, R. R. *J. Chem. Phys.* **1999**, *111*, 6769−6786.

(31) Kim, S.; Wheeler, S. E.; Schaefer, H. F., III *J. Chem. Phys.* **2006**, *124*, 204310.

(32) Aflatooni, K.; Hitt, B.; Gallup, G. A.; Burrow, P. D. *J. Chem. Phys.* **2001**, *115*, 6489−6494.

(33) For example, see: Laenen, R.; Roth, T.; Lambereau, A. *Phys. Rev. Lett.* **2000**, *85*, 50−53.